Structural and Functional Characterisation of Cardiomyocytes Seeded onto 3D PDMS Scaffolds for Myocardial Tissue Engineering

Sara Abou Al-Saud

MRes in Biomedical Research

Imperial College London

Contact: sara.abou-al-saud09@imperial.ac.uk

Supervisor: Dr Patricia Taylor
Co-Supervisor: Dr Kostis Michelakis

Laboratory of Tissue Engineering
Heart Science Centre
National Heart and Lung Institute
Harefield Hospital

5000 words

August 2010

ABSTRACT

Engineering myocardial tissue *in vitro* requires the successful interaction of several essential elements including cells, extracellular matrix (ECM) proteins and three-dimensional (3D) biocompatible scaffolds. In this study a combination of the three elements was used to produce *in vitro* myocardial constructs mimicking *in vivo* cardiac tissue. The novelty of our investigation was the use of synthetic components: 1) novel 3D poly dimethylsiloxane (PDMS) scaffolds for structuring cardiac cell culture and 2) a synthetic fibronectin-mimetic peptide (FMP) for cell-scaffold anchoring. Photolithography was used to fabricate PDMS substrate into a myocardial tissue engineering microgrooved scaffold with several configurations to optimise the geometry support cell alignment and organisation. The same PDMS scaffolds were used for microfluidic application of ECM proteins onto PDMS elastic membranes forming membrane micropatterns. FMP was applied on the microgrooved PDMS scaffolds and micropatterns at different concentrations to optimise the best concentration as a function of cell adhesion. Neonatal rat ventricular myocytes (NRVMs), the most experimentally tested cardiac cells, seeded on these culture structures, developed an *in vivo* like structure and function. In this *in vitro* construct, aligned cardiomyocytes form contacts with other cardiomyocytes via highly organised gap junctions and formed regular sarcomeric patterns visualised by immunohistochemistry, transmission and scanning electron microscopy. FMP was as effective as fibronectin to induce adhesion of the cells in aligned patterns. Spontaneous electrical activity and synchronous calcium (Ca^{2+}) transients of the NRVMs were measured by confocal microscopy. The spontaneous beating rate and the time course of the Ca^{2+} transients were faster in the aligned patterns compared with unstructured cultures, suggesting a functional maturation of NRVMs. These data suggests that 3D PDMS scaffolds and FMP are suitable for tissue engineering cardiac muscle *in vitro*. Further studies are required to assess whether these constructs can be applied *in vivo* to obtain cardiac repair or regeneration.

ABBREVIATIONS

NRVMs	-	Neonatal rat ventricular myocytes
3D	-	Three-dimensional
PDMS	-	Poly dimethylsiloxane
ECM	-	Extracellular matrix
FN	-	Fibronectin
FMP	-	Fibronectin-mimetic peptide
SU8	-	Photoresist polymer
PBS	-	Phosphate buffer saline
FBS	-	Fetal bovine serum
BSA	-	Bovine serum albumin
Ca^{2+}	-	Calcium
SR	-	Sarcoplasmic reticulum
SERCA2	-	Sarcoplasmic reticulum Ca^{2+}-uptake system
NCX	-	Na^{+}/Ca^{2+} exchanger

INTRODUCTION

Heart failure is the final stage of different cardiovascular pathologies, such as myocardial infarction, that leads to myocardial cell death [1]. Adult cardiomyocytes are terminally differentiated and have limited regenerative capacity after infarction [2;3]. This has motivated the rapidly growing interest in developing new cardiac regenerative methods, in order to restore mechanical function of infarcted hearts and prevent or treat heart failure. One proposed approach is to generate patches of cardiac tissue *in vitro*, by seeding cells within biocompatible three-dimensional (3D) scaffolds, to be implanted into damaged hearts [4;5].

One of the main aspects to be considered for generating myocardial tissue is the use of 3D scaffolds that support the mechanical and electrical activities of the heart which are fundamental for cardiac contractility and linked to the highly organised architecture of cardiac cells [6;7]. Therefore, to produce a 3D cardiac tissue construct that preserves both structural and functional characteristics of native cardiac tissue *in vitro*, an optimised scaffold is needed [8-10].

Techniques traditionally have employed culturing cells onto unstructured plastic dishes. This technique often results in a multipolar random array of cells with no significant morphological and electrophysiological properties preserved. More recently, cells have been cultured on scaffolds specifically designed to guide cell alignment and thus cell-to-cell interaction and multicellular organisation [11;12].

Freshly isolated neonatal rat ventricular myocytes (NRVMs) have been used extensively for tissue engineered myocardium by seeding them onto different scaffolds based on its cellular matrix. The cellular matrix stiffness and surface topography greatly affect the cells' morphological maturation and differentiation, and consequently functional behaviour [13]. Scaffolds with non-structured surfaces were used in early studies but these scaffolds, such as collagen-gel scaffolds, demonstrated poor morphogenesis characteristics unless subjected to mechanical stretch [14;15]. Therefore, new *in vitro* protocols for structuring NRVMs culture by using 3D poly dimethylsiloxane (PDMS) microgrooved scaffolds were developed [16-18]. Amongst the various materials employed for tissue engineering, polymers are preferentially used to fabricate scaffolds when considering cost, time and labor [19]. Moreover, PDMS has been the dominant polymeric material utilized as a substrate for microgrooving techniques [20;21]. This can be attributed to its numerous advantages regarding its chemical and physical properties for tissue engineering including its gas permeability, low chemical reactivity, and absence of toxicity for safe *in vivo* implantation [22;23]. In addition it has good flexible properties, making it a suitable scaffold on which to seed contractile cells [24].

However, in all applications, the key step for anchoring cells to the PDMS scaffolds is by treating the surface using extracellular matrix (ECM) proteins. A well-known function of the major ECM proteins, such as collagen and fibronectin (FN), is to provide physical strength to cells and mediate cell shape, cell alignment and cell attachment [12;25;26]. In addition, it is believed that ECM proteins facilitate intercellular electrical coupling and cell-to-cell signalling [26;27]. The ECM proteins currently available are animal-derived which are not suitable for *in vivo* utilization [28]. Thus, the use of synthetic ECM proteins is currently of considerable interest [29]. In recent years there has been substantial effort in designing mimetic peptides as a useful tool for ECM research such as collagen-mimetic peptide [28;29] and fibronectin-mimetic peptide (FMP) [30;31]. Hence, FMP has been widely studied to examine the adhesion property of human umbilical vein endothelial cell [30], prostate cancer cells [32], and colon cancer cells [33]. FMP was tested for the first time in this study for assessing the adhesion of NRVMs onto 3D PDMS scaffolds.

The aim of this study was to use a combination of different PDMS patterns, alteration of FMP concentrations and NRVMs to identify ideal conditions for tissue engineering. The different PDMS patterns were obtained using a set of photolithography, microgrooving and micropatterning

techniques. Firstly, the PDMS scaffolds with 10µm to 100µm microgrooves were constructed by replica-molding the PDMS substrate from microfabricated silicon wafers [34]. Another aspect was optimising the FMP concentration as a function of cell adhesion by using an alternative method of microgrooving on the same PDMS scaffolds. This method produces micropatterns on PDMS flat elastic membrane using microfluidic application of ECM proteins. Such scaffolds for micropatterning have fixed configurations to prevent cell bridging by spacing the 30µm wide lines by 300µm [16;17]. Preserved NRVMs cell morphology, alignment, connectivity and electrical activity were used as parameters to compare the suitability of the different 3D scaffolds for cardiac tissue constructs.

For structural and functional characterisation of seeded NRVMs, both microgrooving and micropatterning protocols were tested using a wide range of techniques, such as light microscopy, immunohistochemistry, scanning electron microscopy and transmission electron microscopy. In addition, the biological functionality of seeded NRVMs was evaluated by electrophysiological investigations focusing on calcium (Ca^{2+}) transient measurements whilst cells were spontaneously beating using confocal microscopy.

MATERIALS AND METHODS

Preparation of fibronectin-mimetic peptide

The structure of the FMP has been previously reported [31;35]. In brief, a peptide-amphiphile (PR-b) was synthesized with a peptide headgroup composed of four building blocks: spacer, the primary binding site for $\alpha_5\beta_1$ integrin (RGDSP), the synergy site (PHSRN) mediating cell adhesion and both connected by a linker. The linker was designed to mimic two important features: the hydrophobicity/ hydrophilicity and the distance between PHSRN and RGD present in natural fibronectin.

- *Structure of FMP*

KSSPHSRNSGSGSGSGSGRGDSP

- *FMP with fluorescent tag*

GGK(*)GGKSSPHSRNSGSGSGSGSGRGDSP
* = Carboxyfluorescein

FMP was synthesized by Fmoc-mediated solid-phase peptide coupling methods and FastMoc chemistry (Applied Biosystems ABI433 peptide synthesiser) from a Gly-preloaded Wang resin (Novabiochem). The peptide was cleaved with a mixture of 95% trifluoroacetic acid, 2.5% triispropylsilane, and 2.5% water for 2.5 hours at room temperature. The volume of the solvent was reduced using a rotary vacuum evaporator. The peptide was triturated with cold diethyl ether, centrifuged and washed several times with fresh diethyl ether, followed by filtration and lyophilisation. The purity of the peptide was checked by reverse-phase high performance liquid chromatography and molecular weight was confirmed by matrix assisted laser desorption/ionisation spectroscopy. FMP was provided by Dr Murugesan Muthu from the Institute of Biomedical Engineering, Imperial College London, UK. FMP was deposited by placing a 20µl of 500µg/ml, 100µg/ml, 50µg/ml, 25µg/ml, 10µg/ml, and 5µg/ml in order to determine the best concentration for cell adhesion.

Preparation of PDMS

- *Photolithography and replica-molding of microgrooved PDMS scaffolds*

Photolithographic patterning of silicon wafers is depicted schematically in **Figure 1**. In brief, a negative photoresist polymer (SU8) was spun onto a silicon wafer (100 mm - diameter). It was then exposed to UV light (365 nm) through a high-resolution transparency glass mask containing 10 to 100μm wide parallel lines and spaced 10 to 300μm apart. Later, the silicon wafer was developed using 100% ethyl lactate as solvent. PDMS was prepared by mixing two components: a base (pre-polymer, PDMS) and a curing agent by 10:1 ratio in weight, respectively (Sylgard 184 Kit, Dow Corning). Before casting onto the SU8 mold, a degassing process was applied to remove any air bubbles. Following casting and curing at 70°C in the oven for 1 hour, the resulting replicas were peeled off leaving deep microgrooves with the specified configurations [16;17;36]. The device fabrication was carried out by Dr Konstantinos Michelakis and Dr Themistoklis Prodromakis in the cleanroom of the Institute of Biomedical Engineering, Imperial College London, UK.

- *Coating of microgrooved PDMS with extracellular matrix proteins*

Microgrooved PDMS were used as scaffolds. A wide range of microgrooved PDMS scaffolds configurations were tested by manipulating the three microgrooves' dimensions using 100-100μm, 100-50μm, 100-20μm, 50-50μm, 50-20μm, 50-10μm, 20-20μm, 20-10μm and 10-10μm as widths (W_1-W_2), and 5.6μm, 4.5μm and 3.78μm as depths (D) **(Figure 2)**. They were washed by immersing them in 70% alcohol twice and placed in petri dishes with the microgrooved surface onto the top. Later, they were rinsed by sterile phosphate-buffered saline (PBS; Oxoid) and exposed to UV light overnight to enhance membrane absorption of ECM proteins. After 24 hours they were coated with different ECM proteins (50μg/ml human-plasma FN (Sigma) or different concentrations of FMP as previously mentioned) by pouring ECM protein containing solutions into the petri dish containing the microgrooved PDMS scaffolds and incubating them for 1 hour at 37C° to allow membrane protein adsorption. Following this, the microgrooved PDMS scaffolds were washed twice with sterile PBS then kept in fresh PBS overnight at 37C° **(Figure 3A).**

- *Micropatterning of extracellular matrix proteins on flat PDMS elastic membrane*

PDMS scaffolds were pressed onto a flat PDMS elastic membrane (Specialty manufacturing Inc., Saginaw, Mi, USA), in contact with the microgrooves [16;17]. The flat PDMS elastic membrane was previously held in a cell culture dish and sterilized by 70% alcohol twice, then rinsed by PBS and kept under UV light overnight. Microfluidic patterning of different ECM proteins was performed by flushing ECM proteins containing solutions (20μl of 50μg/ml FN or different concentrations of FMP) into the formed microgrooves and incubated at 37C° for 1 hour. PDMS scaffolds were finally removed and the dish kept in the incubator for 24 hours **(Figure 3B)**. Microgrooved PDMS scaffolds, that are reusable, were washed between applications using 0.1M acetic acid for 10 minutes to remove any ECM proteins residue from the micropatterns, then sonicated in 70% alcohol for 10 minutes, and exposed to UV light for 5 minutes to dry, prior to any subsequent use.

Cardiomyocyte harvest, seeding and culture

All animal procedures were performed according to the UK Home Office Regulations. NRVMs were isolated and cultured using a method described previously [37]. Hearts were collected from 3-day old neonatal Sprague-Dawley rats after cervical dislocation (Harlan UK Ltd, n= 12 isolations /10-12 hearts each). Ventricles were surgically isolated and minced into 1-2 mm^3 pieces. Cells were dissociated by sequential digestion steps (5 cycles, 15-25 minutes each) shaken at 37°C, using a

mixture of collagenase (Worthington: collagenase Type II, 0.5 mg/ml CLS2) and pancreatin (0.8 mg/ml, Sigma). After each digestion step, cell suspension was collected and resuspended in prewarmed fetal bovine serum (FBS, Invitrogen) for inactivation of enzymes and centrifuged for 5 minutes at 800 rpm. Following this, cells were resuspended in prewarmed FBS and kept in the incubator (37°C, 5% CO2). At the end of the digestion series, all collected cells were centrifuged for 5 minutes at 800 rpm at room temperature.

The cell pellet was resuspended in prewarmed complete medium (Dulbecco's modified Eagle medium, DMEM; Invitrogen) containing 25% medium 199 (M199, Sigma), antibiotics (100 units/ml penicillin, 50 µg/ml streptomycin; Sigma), 15% horse serum (Invitrogen), 7% FBS and 3.4% HEPES (Sigma). The cell suspension was sieved and the fibroblast content was minimized by cell pre-plating into 35mm culture dishes for 45 minutes in the incubator. Myocytes were dislodged from the pre-plated dishes by tapping the dishes several times, whereas the majority of the fibroblasts remained adherent to the plastic. Medium containing the dislodged cardiomyocytes was collected and seeded at a density of 1 million cells per culture dish (60mm) containing micropatterned or microgrooved PDMS. After 24 hours in the incubator, preparations were washed with prewarmed complete medium to remove dead cells and non-adherent cells. Subsequently, medium was exchanged with prewarmed complete medium every 48 hours for 3-5 days before the cells were utilized for experiments.

Experimental testing procedure, data capture, and image analysis

Experiments on viable cultured NRVMs were conducted at room temperature in prewarmed complete medium. All data were recorded within 10-15 minutes. Video microscopy of spontaneously beating NRVMs was accomplished using a Zeiss AxioVert 35 Inverted Microscope coupled to JAI/PULNiX Camera Link ® Cameras capable of video or still imaging mode. Light microscopic observation was performed to assess preferential cell attachment to microfluidically deposited ECM proteins oriented longitudinally into PDMS microgrooves and micropatterns.

Immunohistochemistry staining and imaging

NRVMs structure was determined using immunohistochemistry assay. Firstly, cells attached to PDMS micropatterns (FN and FMP lines) were washed several times with sterile PBS for 3-5 minutes each then fixed with 4% paraformaldehyde for 10 minutes at room temperature. Following this, cells were permeabilized and blocked for 30 minutes in 3% bovine serum albumin (BSA) in PBS containing 0.1% triton X-100. Indirect immunofluorescence was then performed using a panel of antibodies against: sarcomeric α-actin (Sigma), connexin-43 (Invitrogen) and fibronectin antibodies (Invitrogen). Primary antibodies were diluted in 3% BSA in PBS and cell preparations were incubated for 1 hour at room temperature. Subsequently, they were washed 3 times with PBS for 3-5 minutes each, then incubated for 1 hour at room temperature with secondary antibodies (Alexa goat anti-mouse IgM 594 or Alexa goat anti rabbit IgG 488; Invitrogen, diluted 1:1000 in PBS). Preparations were then washed twice with DAPI (Invitrogen, 1:20.000 in PBS) for 3-5 minutes each to stain the cell nuclei. Preparations were mounted in Permaflour mounting medium containing an anti-fade agent (Beckman Coulter). Labelled cells were viewed using an inverted confocal laser scanning microscope (Zeiss Axiovert microscope, Carl Zeiss, Oberkochen, Germany, with an LSM 510 confocal attachment).

Cell adhesion assay to different ECM proteins

The preferential attachment of NRVMs to different ECM proteins micropatterned on PDMS elastic membrane was quantified by determine the ratio of cardiomyocytes to other non-contractile cells. Cells nuclei were stained using the blue-fluorescent DAPI nucleic acid stain and the number of nuclei counted manually using ImageJ software (NIH, USA). The DAPI image was then overlaid on the sarcomeric α-actin image and cells with nuclei that did not overlap with the sarcomeric α-actin stain were considered non-cardiomyocytes.

Scanning electron microscopy

Microgrooved PDMS specimens were fixed in 2.5% glutaraldehyde in 0.1M phosphate buffer for more than two hours followed by 2 buffer washes. The specimens were then post fixed with 1% osmium tetroxide in 0.1M phosphate buffer for 1 hour, washed twice in buffer, incubated with 1% tannic acid in 0.1M phosphate buffer for 1 hour and then washed twice in buffer. Specimens were dehydrated through an ascending series of ethanol applications starting from 25% up to 100% followed by drying with hexamethyldisilazane, then air-dried, mounted on stubs with acheson silver dag and viewed using a JEOL 6600 SEM microscope. All the reagents for scanning electron microscope preparations were obtained from Agar Scientific ltd, Stansted, Essex, UK.

Transmission electron microscopy

Microgrooved PDMS specimens were fixed as previously described in scanning electron microscopy. Specimens were then resin embedded by infiltration with methanol/araldite resin mixture (1:1 ratio) overnight in the specimen rotator. After two more resin changes at least 2 hours in each resin, specimens were placed in plastic petri dishes containing fresh resin and semi-polymerised at 60°C for 3 hours. Beam capsules filled with resin were inverted on to the semi-polymerised fibronectin sheet and polymerised for a further 18 hours. Polymerised beam capsules were teased off from the sheets with the cell layer attached to the resin, trimmed and mounted for sectioning using an Ultracut E microtome. Ultra-thin sections (100 nm) were picked up on formvar coated copper grids. Post staining was carried out by floating the grids on 20 ml droplets of 2% aqueous uranyl acetate and lead citrate solutions. Specimens were viewed using a JEOL 1200 EX microscope (JEOL UK) and digital images were taken using a digital micrograph camera (Gatan UK).

Imaging of cell structure and Ca^{2+} transients using confocal microscopy

To visualise the structure of NRVMs aligned on both micropatterned and microgrooved PDMS, NRVMs were incubated with Di-8-ANEPPS (10μM, Molecular Probes, Eugene, OR, USA) for 10 minutes, and then washed with prewarmed complete medium. For Ca^{2+} transients' identification NRVMs were loaded with Rhod-2 AM (30μM, Invitrogen) at room temperature in the dark for 30 minutes, then washed again using prewarmed complete medium and left for at least 30 minutes to de-esterify. Di-8-ANEPPS and Rhod-2 AM were excited at 488-nm and 552-nm, and the emitted fluorescence was collected through 505-nm and 581-nm long-pass filters, respectively. NRVMs were studied using the same confocal microscope described previously.

To measure Ca^{2+} transient morphology, a line scan was performed whilst NRVMs were beating spontaneously. Time-to-peak was taken as the time taken for the ratio signal to go from baseline fluorescence to peak fluorescence; baseline fluorescence emission was taken as an index of diastolic Ca^{2+} concentration; peak fluorescence emission was taken as an index of systolic Ca^{2+} concentration and Ca^{2+} transient amplitude was defined as the peak fluorescence over baseline fluorescence. Synchronicity of Ca^{2+} release was assessed as the variance of time-to-peak amplitude; 50% and 90% decay were the time taken for the Rhod-2 AM Ca^{2+} transient to decline by 50% as well as 90% of the transient amplitude from peak fluorescence, as previously described [38] **(Figure 4)**. The analysis was performed using custom-written routines in MATLAB R2006 (The MathWorks, Inc.). Spontaneous beating rate was assessed by manually counting the number of Ca^{2+} transients per specific period of time.

Statistical analysis

Data are expressed as mean ± SEM, and analysed using one-way ANOVA test followed by post Bonferroni test, except where indicated. The analysis was performed using Prism4 software (GraphPad Software Inc., San Diego, CA, USA). *P* values<0.05 (95% confidence level) were considered significant.

RESULTS

Optimisation of microgrooved PDMS scaffold topography and FMP concentration

A wide range of microgrooved PDMS scaffold configurations ranging from 10µm to 300µm were tested and it was found that 20-10-4.5µm (W_1-W_2-D) were the best dimensions for controlling cell alignment and organisation **(Figure 5)**. In addition, microgrooved PDMS scaffolds were used to pattern alternating high and low concentrations of FMP protein (FN was used as a control). PDMS flat elastic membrane that had been inked with a 20µl droplet of 50µg/ml FMP showed comparable adhesion property with PDMS micropatterned with 50µg/ml FN. The percentage of cells adherent to micropatterned PDMS using FN was 51.18±5.93% whereas for FMP it was 47.83 ± 3.71% (no significant differences detected using student t-test, *P*>0.05, n=10).

Light microscopic observation showed no clear difference in NRVMs structure seeded onto micropatterned PDMS lines using different ECM proteins **(Figure 6)**. High-resolution confocal scanning microscope observation of FN and FMP micropatterned on PDMS elastic membrane showed continuous lines of ECM proteins with the specific concentration of ECM solutions used (data not shown). Adherence of NRVMs to FMP coated microgrooved PDMS was not observed. Further studies using the fluorescently tagged FMP revealed that although FMP adhered to flat PDMS elastic membrane, it did not adhere to microgrooved PDMS scaffold (data not shown). Thus FMP could not be used for studies with microgrooved PDMS scaffolds.

Cell shape, morphology and organisation

NRVMs were cultured on patterned (microgrooved and micropatterned PDMS) and non-patterned surfaces under the same conditions for comparison. During days 1-2 in culture, NRVMs seeded onto PDMS patterned substrate acquired a physiological, elongated and aligned morphology after adherence to FN-coated microgrooves and FN and FMP micropatterns. On the other hand, NRVMs seeded onto unpatterned substrate showed no preferential alignment with multipolar cell shape. Examination by light microscopy showed that NRVMs adhered to FN-coated PDMS microgrooves **(Figure 5)** and FN or FMP micropatterns **(Figure 6)** developed a uniaxial organisation and alignment of NRVMs with morphology resembling native cardiac tissue structure in a reproducible pattern. 72 hours after seeding, NRVMs were closely approximating each other and spontaneous contraction of single cells was observed. After 4 days in culture, coordinated contraction of the entire aligned NRVMs population was recorded. Cells remained viable in culture for 2 weeks.

The visualisation of membranous and cytoskeleton architecture of NRVMs seeded onto both patterned PDMS was determined by fluorescent confocal imaging using Di-8-ANEPPS **(Figure 7).** In addition, NRVMs seeded onto PDMS FN micropatterns studied by immunohistochemistry staining showing NRVMs grown on FN lines showing elongated shape **(Figure 8)** with highly organised gap junctions in between cells (data not shown). A possible attachment between NRVMs seeded onto microgrooved PDMS scaffold was detected above the aligned microgrooved layer **(Figure 9)**. High resolution images captured using scanning electron microscopy demonstrated cellular communication between aligned NRVMs through gap junctions' formation **(Figure 10A)**. In addition, the formation of a cardiac tissue layer from NRVMs seeded onto microgrooved PDMS scaffold is depicted in

Figure 10B. The sarcomeres, composed of an array of overlapping thick and thin filaments between two adjacent Z discs, were clearly visible using transmission electron microscope in aligned NRVMs **(Figure 11)**.

Functional properties of patterned and unpatterned cells

To test whether controlling cell culture structure altered Ca^{2+} transient morphology, NRVMs seeded in FN coated microgrooved PDMS scaffolds **(Figure 12)**, FN and FMP micropatterned PDMS and unpatterned PDMS were stained with Rhod-2 AM. NRVMs seeded in unpatterned PDMS served as controls. NRVMs were spontaneously beating while recording line scans. In aligned NRVMs seeded into microgrooved and micropatterned PDMS, the average time-to-peak was significantly shorter **(***P*<0.0001**, Table 1, Figure 13A)** as was the time to 50% decay (*P*<0.0001, **Figure 13B**) compared with control cells. The peak amplitude of NRVMs seeded on patterned and unpatterned PDMS showed no significant difference (*P*>0.05, **Figure 13C**) nor were there differences in the time to 90% decay (*P*>0.05, **Figure 13D**). The synchronicity of Ca^{2+} release was significantly greater in aligned cells **(***P*<0.0001**, Figure 13E)**. Estimation of spontaneous beat rate was obtained from NRVMs Ca^{2+} measurements and showed a very slow beat rate in control NRVMs (26 beats/ minute) with a significantly faster (3-4 folds) rate in NRVMs seeded on patterned PDMS (*P*<0.0001, **Table 1**).

DISCUSSION

The aim of this study was to optimise the geometry of microgrooved PDMS scaffolds for controlling cell culture structure of NRVMs. Further optimization of microenvironment conditions was attempted by optimising the concentration of synthetic FMP. This allowed for NRVMs to be seeded within an *in vitro* 3D construct that developed structural and functional parameters suitable for *in vivo* implantation into damaged heart. Growing NRVMs onto defined topography of microgrooved PDMS scaffolds as well as PDMS micropatterns was successful and produced significant results regarding NRVMs' structure and function.

Giving the relatively lack of toxicity of PDMS scaffolds for NRVMs, it is likely that the construct described in this paper can be the first step towards the development of cell-scaffold system with modified geometry for cell alignment, fabricated from biodegradable materials suitable for *in vivo* use in the future [39]. We found that 20-10-4.5µm (W_1-W_2-D) dimensions were the best after testing a wide range of configurations. In addition, the PDMS micropatterns showed similar results using 30µm wide lines. These arrangements allowed the linear seeding of NRVMs that would lack structure and morphology when grown in an unpatterned culture dish. These specific geometries in accordance with previous studies showing that the radius of each cardiomyocyte is about 10.5µm which is similar to our optimal microgrooved PDMS scaffold width (W_1) and PDMS micropatterns [40].

Although it is difficult to mimic the structure of native fibronectin, the FMP used in this study performed comparably to fibronectin in terms of promoting cell adhesion. It has been reported to have similar characteristics to fibronectin by others [30-33;35;41]. One unexpected result was the non-adherence of FMP to microgrooved PDMS scaffolds. The failure of this adhesiveness may reflect low surface energy of the microgrooved PDMS scaffold preventing the surface from successful bonding to FMP. There are numerous techniques for improving surface functionality and one possible solution could be oxygen-plasma treatment. It is a surface roughening method to obtain optimal bond strength which can be tested in future studies for microgrooved PDMS scaffolds and FMP adhesion [15;42;43].

The resultant *in vitro* construct showed characteristic rod-shaped morphology of cardiomyocytes, connected by gap junctions and intercalated discs with regular arrangement of sarcomeres. All were

organized by ECM proteins into microgrooved and micropatterned PDMS comparable to cells in intact myocardial tissue **(Figures 4-9,** see also [44;45]**)**. Previous studies by Camelliti *et al.* using similar micropatterned and microgrooved PDMS scaffolds treated with animal-derived ECM proteins showed results consistent with our data [16;17].

There is accumulating evidence that the highly regular arrangement of NRVMs produced in structured tissue cultures, associated with the improved cellular gap junction organisation and thus electrical connectivity between cells, improves Ca^{2+} handling hence cell contractility [46;47] . To test the hypothesis that manipulating cell arrangement might promote biomimetic functionality, intracellular Ca^{2+} handling parameters were assessed; Ca^{2+} transient parameters were altered in spontaneously beating NRVMs seeded on patterned (microgrooved and micropatterned) PDMS compared with un-patterned PDMS **(Figure 13)**. A potential problem was discovered during this experiment, that NRVMs may form junctions above the aligned microgrooved layer and this can affect the function of the construct. The interpretation of the possible communication between NRVMs is the lack of scaffolds' depth which may affect some of the results **(Figure 9)**. We focused only on aligned cells in PDMS microgrooves in our measurements despite the existence of possible overlapping across the microgrooves.

Depolarisation of the myocyte sarcolemma causes the opening of both fast Na^{+} and L-type Ca^{2+} channels. The 'long-lasting' L-type Ca^{2+} channel is the major pathway for Ca^{2+} entry into the cell. The initial Ca^{2+} through L-type channels acts as a 'trigger' for release of Ca^{2+} from the sarcoplasmic reticulum (SR) via the ryanodine receptors. This process is termed calcium-induced-calcium-release. Once Ca^{2+} is released from the SR, free Ca^{2+} in the cytosol binds to myofilaments inducing contraction [48;49]. In our study, Ca^{2+} transients were detected by visualising fluorescence changes of the Ca^{2+}-sensitive dye Rhod-2 AM. We measured Ca^{2+} transient amplitude which was unchanged between aligned and unaligned NRVMs, whereas time-to-peak was faster in aligned compared to unaligned NRVMs. This could indicate functional maturation in NRVMs seeded onto aligned patterns with more synchronous release of Ca^{2+} from SR.

Relaxation is essential for cardiac function, and is mediated by the rapid removal of Ca^{2+} from the cytosol during the repolarisation phase through: 1) re-accumulating Ca^{2+} into the SR by active pumping through the sarcoplasmic reticulum Ca^{2+}-uptake system (SERCA2) and 2) to extracellular space by passive exchange via the Na^{+}/Ca^{2+} exchanger (NCX) (**Figure 14**, see also [49]). We measured time to 50% as well as 90% decay of Ca^{2+} transients. Time to 50% decay was faster in aligned NRVMs, whereas no differences were shown by the time to 90% decay. We speculate that the changes might be due to the differences in Ca^{2+} handling proteins linked to either the time course of Ca^{2+} release and entry to the SR or the rate of NCX function which has non-linear relationship with SERCA2 activity, especially towards the end of the relaxation phase (for relative contribution see [50]). These changes may also indicate a functional maturation of the NRVMs in aligned patterns.

We conclude that manipulating cell culture structure by modifying scaffold geometry and adhesive properties is essential to the development of 3D constructs with myocardial-like structure and function, which better mimics electrophysiology of native myocardium.

FUTURE RESEARCH

Further work includes enhancing this study by increasing the number of experiments regarding Ca^{2+} transients' measurements. Furthermore, the microelectrode technique and optical mapping system will be applied for action potential measurements, as well as to assess the environmental influences on drug efficacy in highly structured cardiac cultures. Cardiomyocytes derived from other sources such as human embryonic stem cells and induced pluripotent stem cells will be seeded in microgrooved PDMS scaffolds *in vitro.* Following that, cell-scaffold systems will be implanted *in vivo* and functional integration will be investigated together with the ability to improve heart function after injury.

ACKNOWLEDGMENTS

I am grateful to my supervisor Dr Patricia Taylor for her guidance and support in this study, Dr Kostis Michelakis and Dr Themistoklis Prodromakis for PDMS scaffolds fabrication, Dr Cesare Terracciano for his critical reading of this manuscript and insightful discussion, Dr Patrizia Camelliti who contributed to the development of the protocols, Dr Padmini Sarathchandra for her fundamental contribution regarding the structural studies carried out in this work, Dr Murugesan Muthu for providing FMP and fluorescently tagged FMP, and Dr Urszula Siedlecka for Ca^{2+} transient analysis studies. Funding was generously provided by King Saud University, King Fahad Cardiac Centre and The Magdi Yacoub Institute.

Reference List

1 Whelan, R. S., Kaplinskiy, V., and Kitsis, R. N. (2010) Annu.Rev.Physiol **72**, 19-44

2 Bergmann, O., Bhardwaj, R. D., Bernard, S., Zdunek, S., Barnabe-Heider, F., Walsh, S., Zupicich, J., Alkass, K., Buchholz, B. A., Druid, H., Jovinge, S., and Frisen, J. (2009) Science **324**, 98-102

3 Schussler, O., Chachques, J. C., Mesana, T. G., Suuronen, E. J., Lecarpentier, Y., and Ruel, M. (2010) Asian Cardiovasc.Thorac.Ann. **18**, 188-198

4 Yeong, W. Y., Sudarmadji, N., Yu, H. Y., Chua, C. K., Leong, K. F., Venkatraman, S. S., Boey, Y. C., and Tan, L. P. (2010) Acta Biomater. **6**, 2028-2034

5 Giraud, M. N., Ayuni, E., Cook, S., Siepe, M., Carrel, T. P., and Tevaearai, H. T. (2008) Artif.Organs **32**, 692-700

6 Valderrabano, M. (2007) Prog.Biophys.Mol.Biol. **94**, 144-168

7 Coghlan, H. C., Coghlan, A. R., Buckberg, G. D., and Cox, J. L. (2006) Eur.J.Cardiothorac.Surg. **29 Suppl 1**, S178-S187

8 Radisic, M., Park, H., Gerecht, S., Cannizzaro, C., Langer, R., and Vunjak-Novakovic, G. (2007) Philos.Trans.R.Soc.Lond B Biol.Sci. **362**, 1357-1368

9 Eschenhagen, T. and Zimmermann, W. H. (2005) Circ.Res. **97**, 1220-1231

10 McDevitt, T. C., Woodhouse, K. A., Hauschka, S. D., Murry, C. E., and Stayton, P. S. (2003) J.Biomed.Mater.Res.A **66**, 586-595

11 Rockwood, D. N., Akins, R. E., Jr., Parrag, I. C., Woodhouse, K. A., and Rabolt, J. F. (2008) Biomaterials **29**, 4783-4791

12 Eitan, Y., Sarig, U., Dahan, N., and Machluf, M. (2010) Tissue Eng Part C.Methods **16**, 671-683

13 Jacot, J. G., Kita-Matsuo, H., Wei, K. A., Chen, H. S., Omens, J. H., Mercola, M., and McCulloch, A. D. (2010) Ann.N.Y.Acad.Sci. **1188**, 121-127

14 Robert Paul Lanza, Robert S.Langer, and Josef Vacanti (1997) In Principles of tissue engineering

15 Birla, R. K., Huang, Y. C., and Dennis, R. G. (2007) Tissue Eng **13**, 2239-2248

16 Camelliti, P., McCulloch, A. D., and Kohl, P. (2005) Microsc.Microanal. **11**, 249-259

17 Camelliti, P., Gallagher, J. O., Kohl, P., and McCulloch, A. D. (2006) Nat.Protoc. **1**, 1379-1391

18 Feinberg, A. W., Feigel, A., Shevkoplyas, S. S., Sheehy, S., Whitesides, G. M., and Parker, K. K. (2007) Science **317**, 1366-1370

19 Zhou, J., Ellis, A. V., and Voelcker, N. H. (2010) Electrophoresis **31**, 2-16

20 McDonald, J. C. and Whitesides, G. M. (2002) Acc.Chem.Res. **35**, 491-499

21 McDonald, J. C., Duffy, D. C., Anderson, J. R., Chiu, D. T., Wu, H., Schueller, O. J., and Whitesides, G. M. (2000) Electrophoresis **21**, 27-40

22 Regehr, K. J., Domenech, M., Koepsel, J. T., Carver, K. C., Ellison-Zelski, S. J., Murphy, W. L., Schuler, L. A., Alarid, E. T., and Beebe, D. J. (2009) Lab Chip. **9**, 2132-2139

23 Zhou, J., Ellis, A. V., and Voelcker, N. H. (2010) Electrophoresis **31**, 2-16

24 Kuncova-Kallio, J. and Kallio, P. J. (2006) Conf.Proc.IEEE Eng Med.Biol.Soc. **1**, 2486-2489

25 Little, C. D. and Rongish, B. J. (1995) Experientia **51**, 873-882

26 Bowers, S. L., Banerjee, I., and Baudino, T. A. (2010) J.Mol.Cell Cardiol. **48**, 474-482

27 Pelouch, V., Dixon, I. M., Golfman, L., Beamish, R. E., and Dhalla, N. S. (1993) Mol.Cell Biochem. **129**, 101-120

28 Koide, T. (2007) Philos.Trans.R.Soc.Lond B Biol.Sci. **362**, 1281-1291

29 Goodman, M., Bhumralkar, Jefferson, E. A., Kwak, J., and Locardi, E. (1998) Biopolymers **47**, 127-142

30 Craig, J. A., Rexeisen, E. L., Mardilovich, A., Shroff, K., and Kokkoli, E. (2008) Langmuir **24**, 10282-10292

31 Rexeisen, E. L., Fan, W., Pangburn, T. O., Taribagil, R. R., Bates, F. S., Lodge, T. P., Tsapatsis, M., and Kokkoli, E. (2010) Langmuir **26**, 1953-1959

32 Demirgoz, D., Garg, A., and Kokkoli, E. (2008) Langmuir **24**, 13518-13524

33 Garg, A., Tisdale, A. W., Haidari, E., and Kokkoli, E. (2009) Int.J.Pharm. **366**, 201-210

34 Ainslie, K. M. and Desai, T. A. (2008) Lab Chip. **8**, 1864-1878

35 Mardilovich, A., Craig, J. A., McCammon, M. Q., Garg, A., and Kokkoli, E. (2006) Langmuir **22**, 3259-3264

36 McDonald, J. C. and Whitesides, G. M. (2002) Acc.Chem.Res. **35**, 491-499

37 Brand, N. J., Lara-Pezzi, E., Rosenthal, N., and Barton, P. J. (2010) Methods Mol.Biol. **633**, 113-124

38 Stagg, M. A., Carter, E., Sohrabi, N., Siedlecka, U., Soppa, G. K., Mead, F., Mohandas, N., Taylor-Harris, P., Baines, A., Bennett, P., Yacoub, M. H., Pinder, J. C., and Terracciano, C. M. (2008) Circ.Res. **103**, 855-863

39 Simmons, A., Hyvarinen, J., Odell, R. A., Martin, D. J., Gunatillake, P. A., Noble, K. R., and Poole-Warren, L. A. (2004) Biomaterials **25**, 4887-4900

40 Korhonen, T., Hanninen, S. L., and Tavi, P. (2009) Biophys.J. **96**, 1189-1209

41 Bartsch, J. E., Staren, E. D., and Appert, H. E. (2003) J.Surg.Res. **110**, 383-392

42 Rizzi, G., Scrivani, A., Fini, M., and Giardino, R. (2004) Int.J.Artif.Organs **27**, 649-657

43 Oppegard, S., Sinkala, E., and Eddington, D. (2010) J.Vis.Exp.

44 Lunkenheimer, P. P., Redmann, K., Kling, N., Jiang, X., Rothaus, K., Cryer, C. W., Wubbeling, F., Niederer, P., Heitz, P. U., Ho, S. Y., and Anderson, R. H. (2006) Anat.Rec.A Discov.Mol.Cell Evol.Biol. **288**, 565-578

45 LeGrice, I. J., Smaill, B. H., Chai, L. Z., Edgar, S. G., Gavin, J. B., and Hunter, P. J. (1995) Am.J.Physiol **269**, H571-H582

46 Desplantez, T., Dupont, E., Severs, N. J., and Weingart, R. (2007) J.Membr.Biol. **218**, 13-28

47 Yin, L., Bien, H., and Entcheva, E. (2004) Am.J.Physiol Heart Circ.Physiol **287**, H1276-H1285

48 duBell, W. H., Boyett, M. R., Spurgeon, H. A., Talo, A., Stern, M. D., and Lakatta, E. G. (1991) J.Physiol **436**, 347-369

49 Benitah, J. P., Alvarez, J. L., and Gomez, A. M. (2010) J.Mol.Cell Cardiol. **48**, 26-36

50 Bers, D. M. (2002) In Excitation-Contraction Coupling and Cardiac Contractile Force pp. 63-100, Springer,

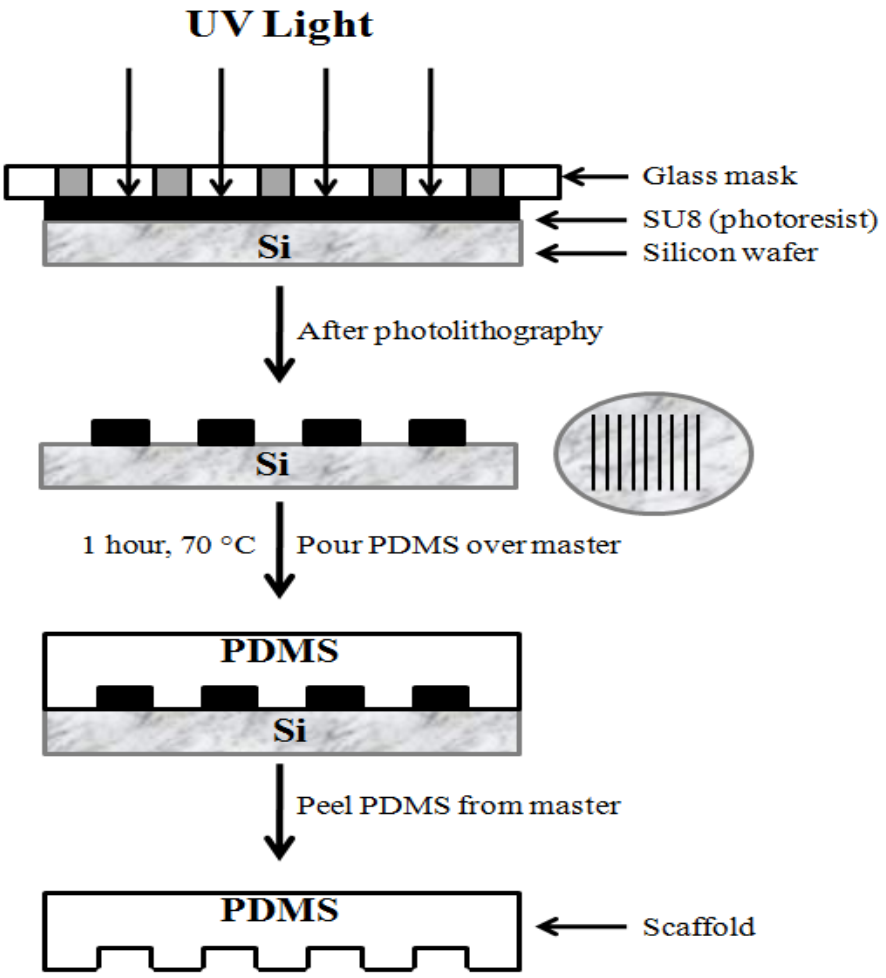

Figure 1. Scheme shows Photolithography and PDMS fabrication process.

The silicon wafer was spin coated by SU8 photoresist then exposed to UV light through a glass mask with different µm configurations. Various micropatterns were developed on the silicon master to be used as a template for PDMS replication device.

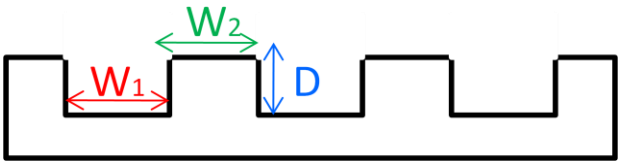

Figure 2. Manipulating microgrooved PDMS scaffold configurations.

W_1 indicates the groove's width (red arrow), W_2 indicates the top's width (green arrow) and D indicates the depth (blue arrow), of the fabricated PDMS substrate. 100µm, 50µm, 20µm and 10µm were tested for W_1 and W_2, whereas 3.78µm, 4.5µm and 5.6µm were tested for depths.

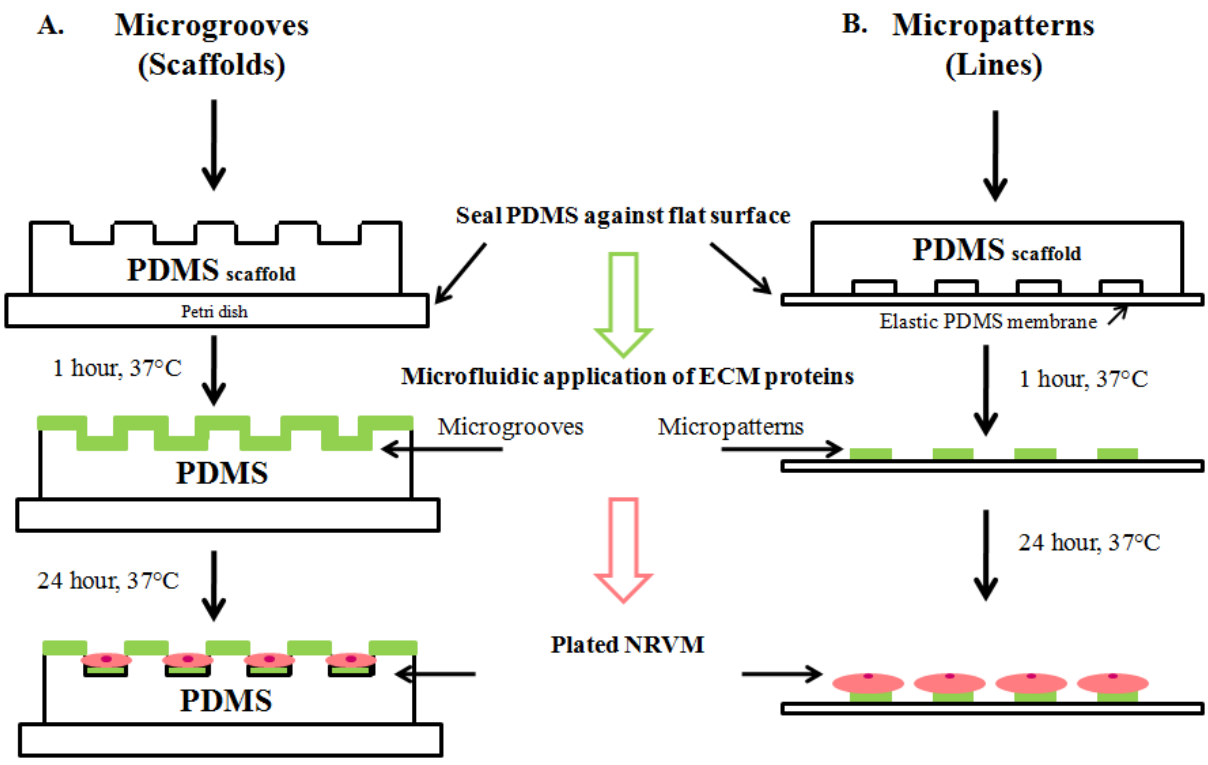

Figure 3. Microfluidic application of different ECM proteins onto PDMS scaffolds showing cell growth only on lines and grooves.

A. Coated microgrooved PDMS scaffolds. **B.** Micropatterned ECM line formation on a flat PDMS elastic membrane (parallel lines, 30µm in width, 300µm apart and 2cm in length).

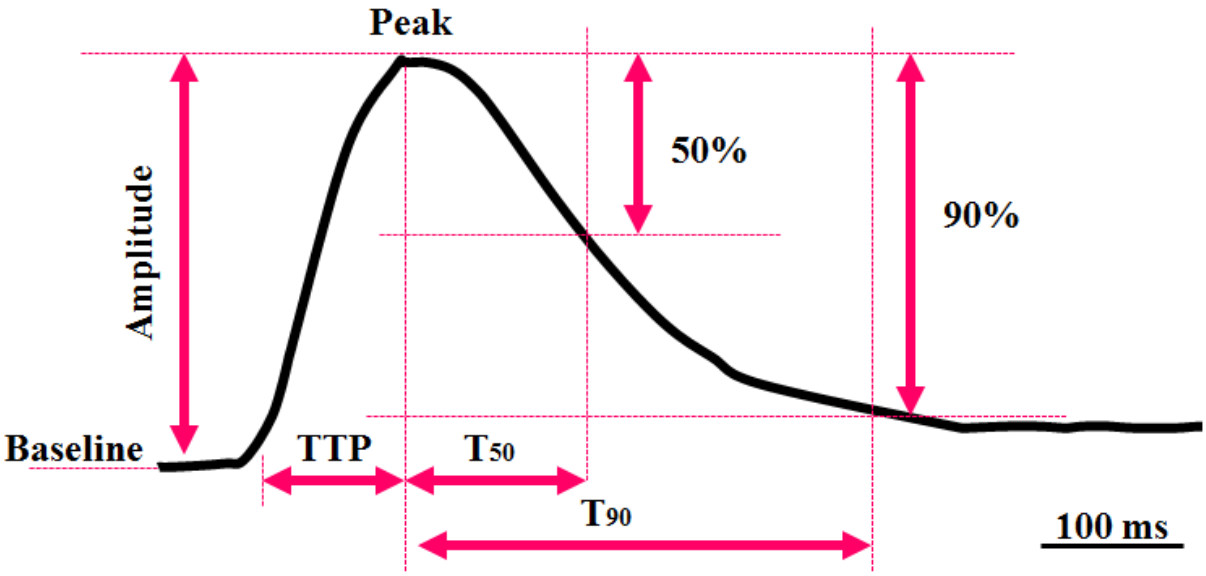

Figure 4. Parameters analysed from the Rhod-2 Ca^{2+} transients.

Analysis was performed using the time taken for the ratio signal to go from baseline fluorescence to peak fluorescence as the time-to-peak (TTP); the peak fluorescence over baseline fluorescence as Ca^{2+} transient amplitude; the variance of TTP amplitude as the synchronicity of Ca^{2+} release and the time taken for the Rhod-2 AM transient to decline by 50% as well as 90% of the transient amplitude from peak fluorescence as 50% (T_{50}) and 90% (T_{90}) decay.

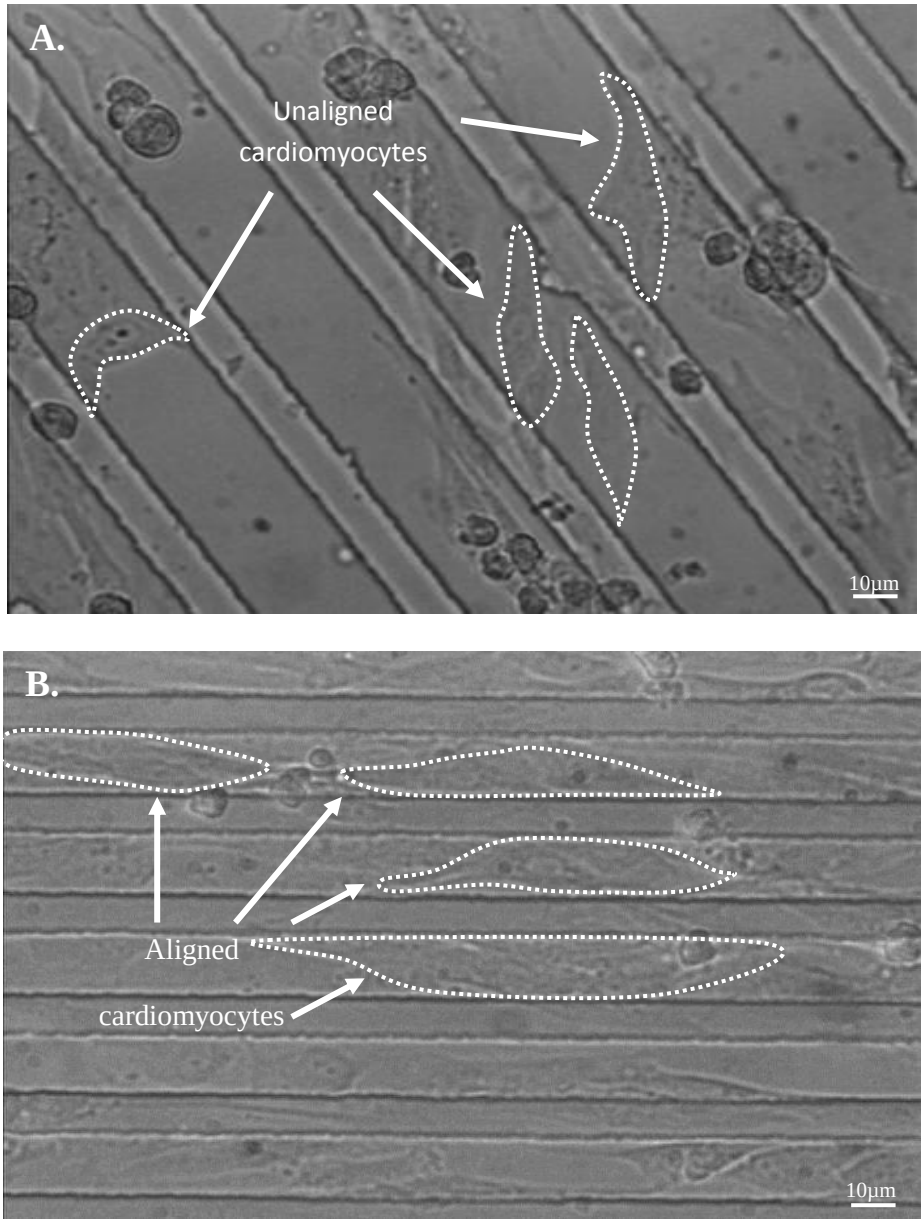

Figure 5. Light micrographs (40x) show NRVMs seeded onto microgrooved PDMS scaffolds with different configurations.

Cells do not align following the geometry of the 50-10-4.5µm (W_1-W_2-D) microgrooved PDMS scaffold **(A.)**; whereas cells align in 20-10-4.5µm microgrooved PDMS scaffold **(B.)**.

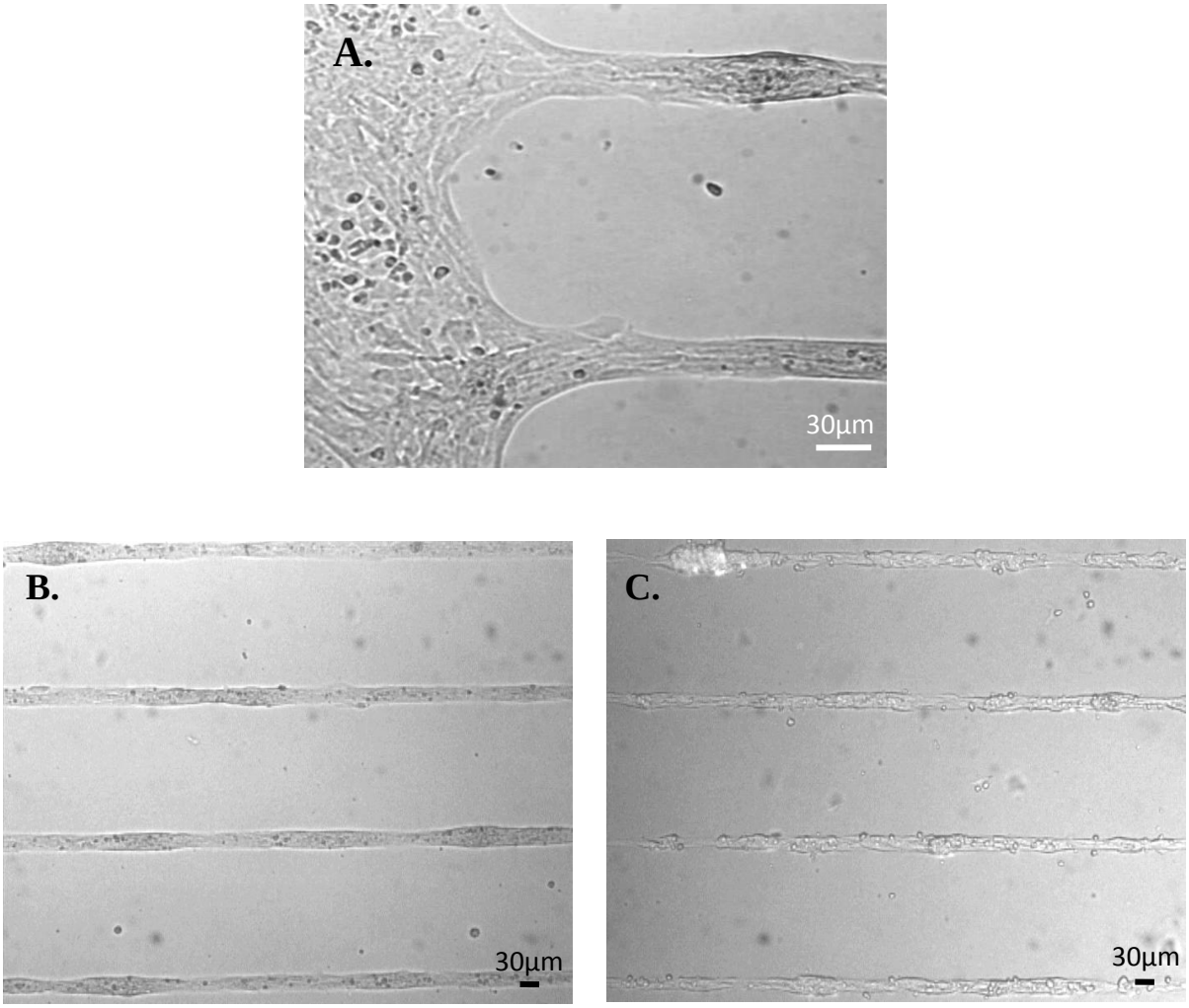

Figure 6. NRVMs seeded onto micropatterned FN and FMP protein lines.

A. Preferential cell attachment to microfluidically deposited ECM proteins (right half of **A.**) and the randomly distributed cells in the nonpatterned culture region (left half of **A.**). Micropatterns of 30µm wide lines spaced 300µm apart producing a uniaxial array of seeded NRVMs using 50µg/ml FN (**B.)** and 50µg/ml FMP (**C.)**.

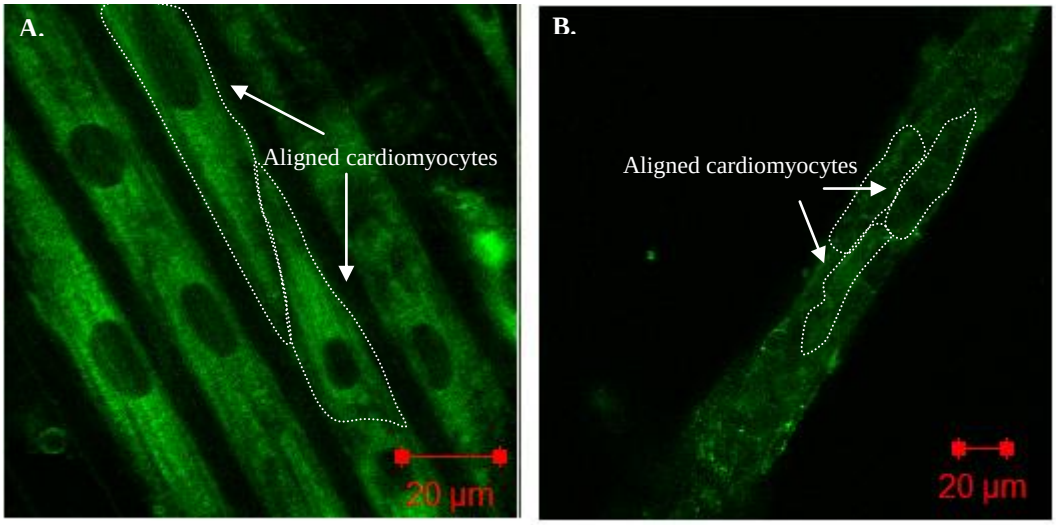

Figure 7. The visualisation of membranous and cytoskeleton architecture of NRVMs seeded onto both patterned PDMS determined by fluorescent confocal imaging using Di-8-ANEPPS.

NRVMs aligned in 20-10-4.5µm microgrooves **(A.)** and micropatterns **(B.)** anchored by FN showing elongated morphology of NRVMs at day 3.

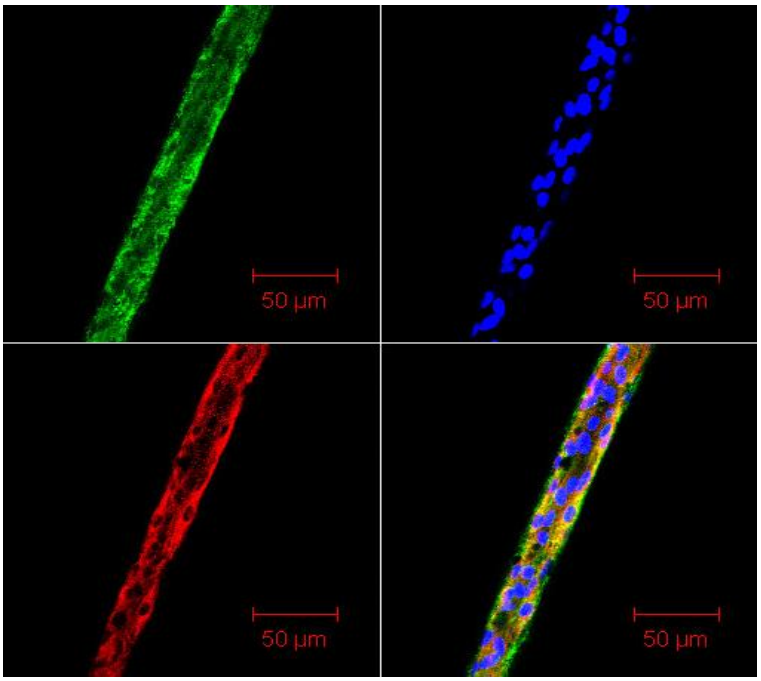

Figure 8. The alignment of NRVMs seeded onto micropatterned FN lines and verified by the immunohistochemistry staining.

Images show stained cardiomyocytes (red), nuclei (blue) and fibronectin (green).

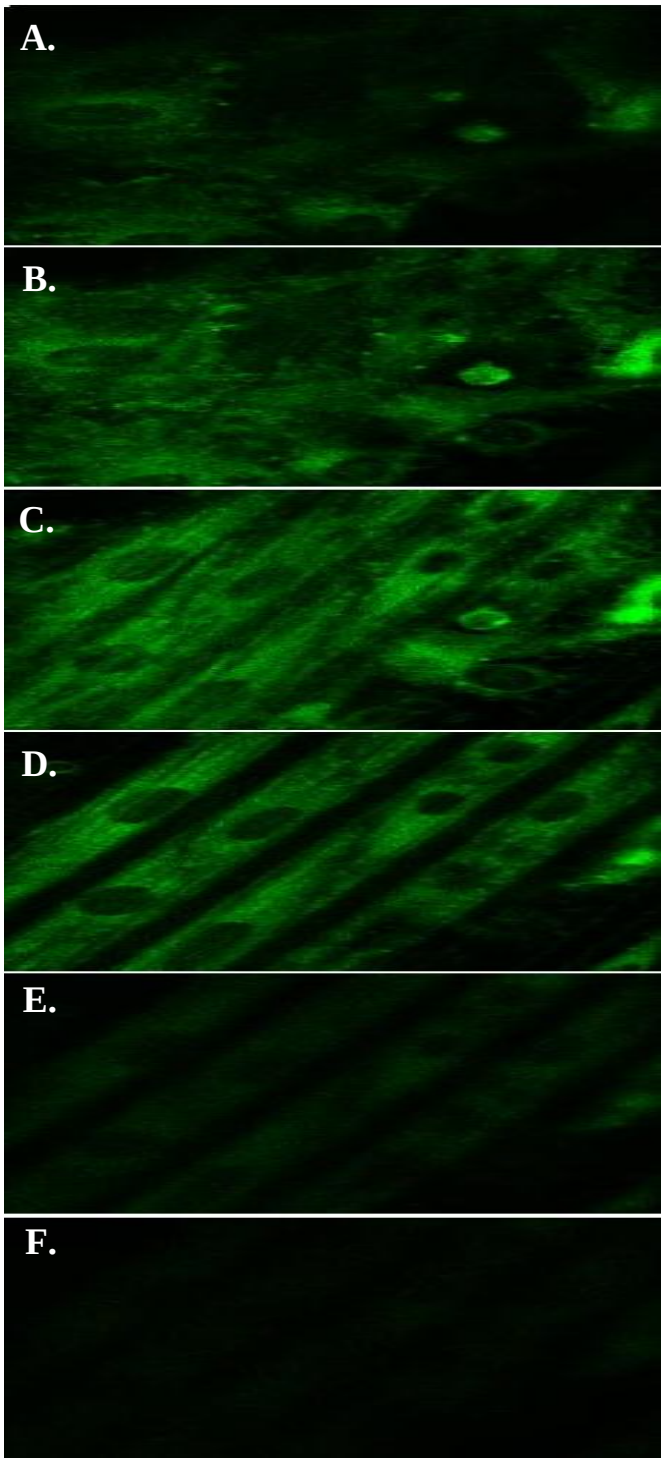

Figure 9. Series of z-axis confocal images (top to bottom) with 4µm interval in between showing an existing overlapping between NRVMs seeded into 20-10-4.5µm microgrooved PDMS scaffolds.

Fluorescent confocal image (40x) for NRVMs loaded with Di-8-ANEPPS (10µM) showing that many cells are in contact , on the top and across the microgroove openings, **(A.-C.)**, whereas a well defined structure of NRVMs detected within the PDMS microgrooves' W_1 **(D.-F.)**.

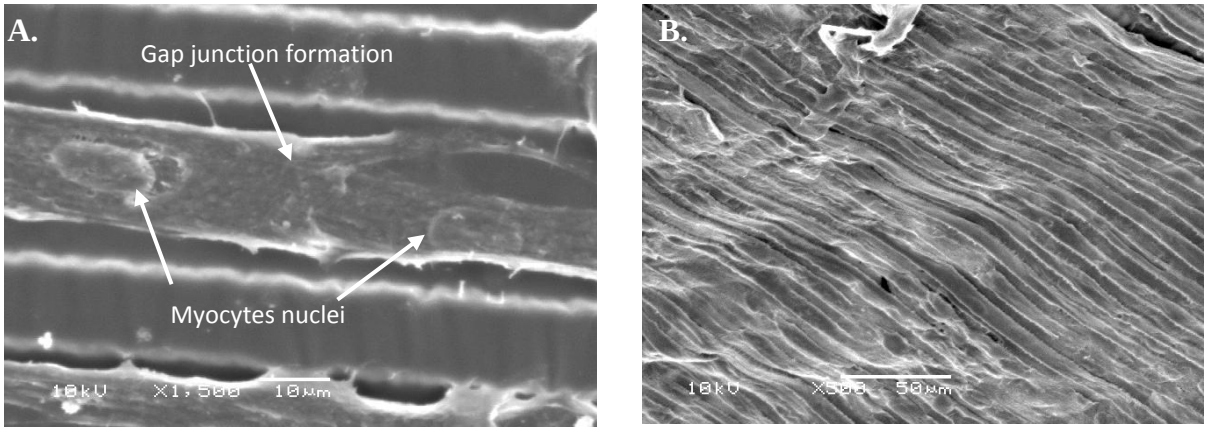

Figure 10. Scanning electron micrographs showing NRVMs seeded onto microgrooved PDMS scaffolds.

A. The higher magnification image shows the alignment of cardiomyocytes in PDMS microgrooves (20-10-4.5µm) and the interconnection between cells via gap junction formation at day 3. Note cells are restricted to the bottom of the microgroove (W_1). **B.** The lower magnification image shows the formation of a confluent myocardial layer at day 5**.**

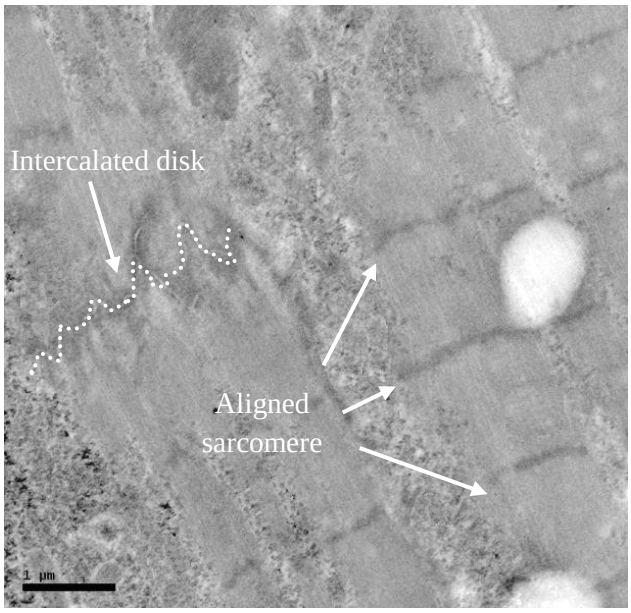

Figure 11. Transmission electron micrograph shows sarcomere organization and intercalated disk formation between NRVMs seeded into 20-10-4.5µm microgrooved PDMS scaffolds.

The geometry of microgrooved PDMS scaffold influenced myocyte alignment and organization leading to sarcomere alignment by directing the actin network orientation.

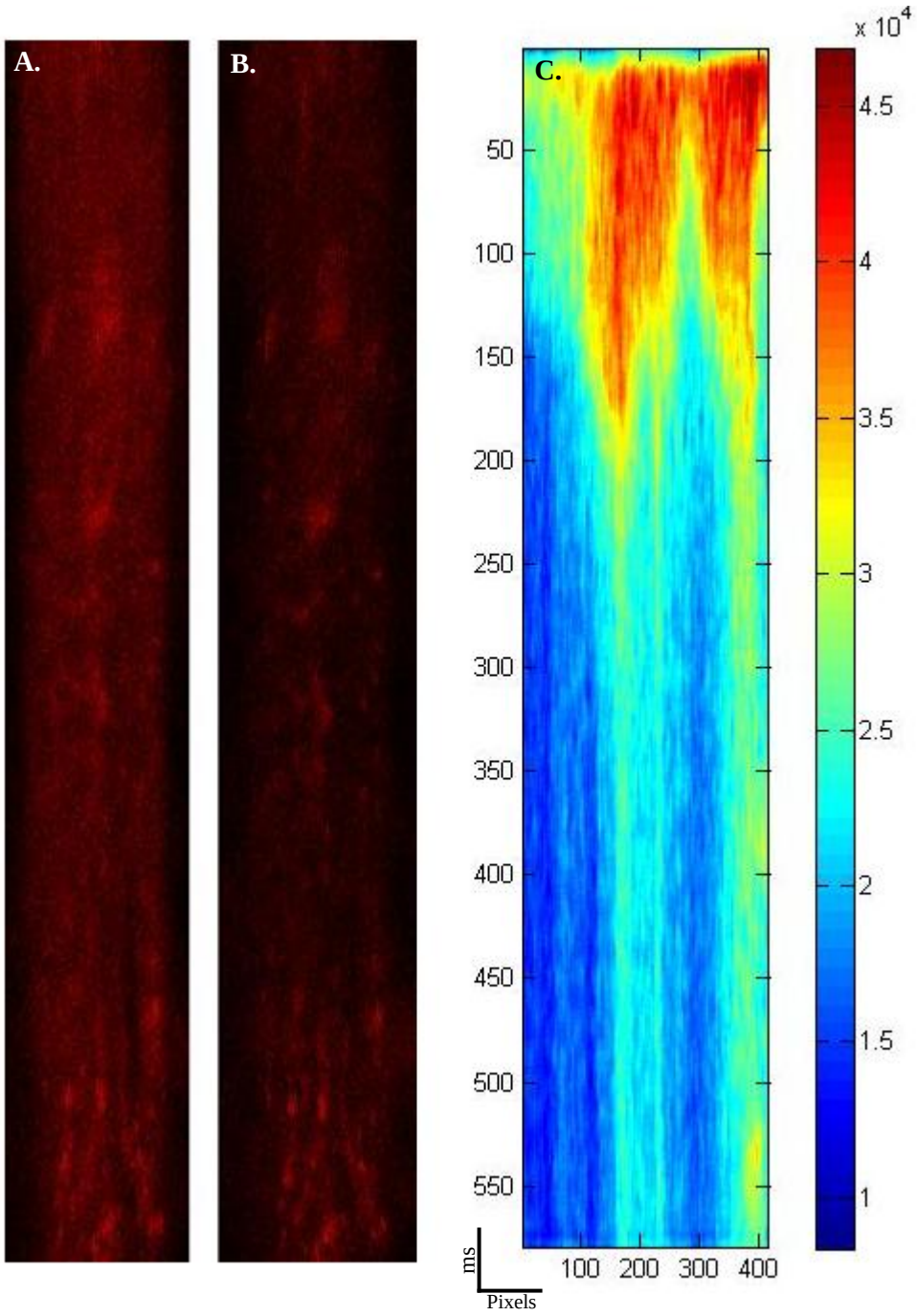

Figure 12. Ca^{2+} transient in spontaneously beating NRVMs seeded into 20-10-4.5µm microgrooved PDMS scaffolds.

Fluorescent confocal image (40x) showing aligned NRVMs loaded with Rhod-2 AM for intracellular Ca^{2+} measurements. Increase in cytoplasmic Ca^{2+} concentration following cell membrane depolarisation is indicated by higher red fluorescence **(A.)** in comparison to repolarisation phase **(B.). (C.)** A representative trace shows a Ca^{2+} transient in spontaneously beating aligned NRVMs measured in line scan mode.

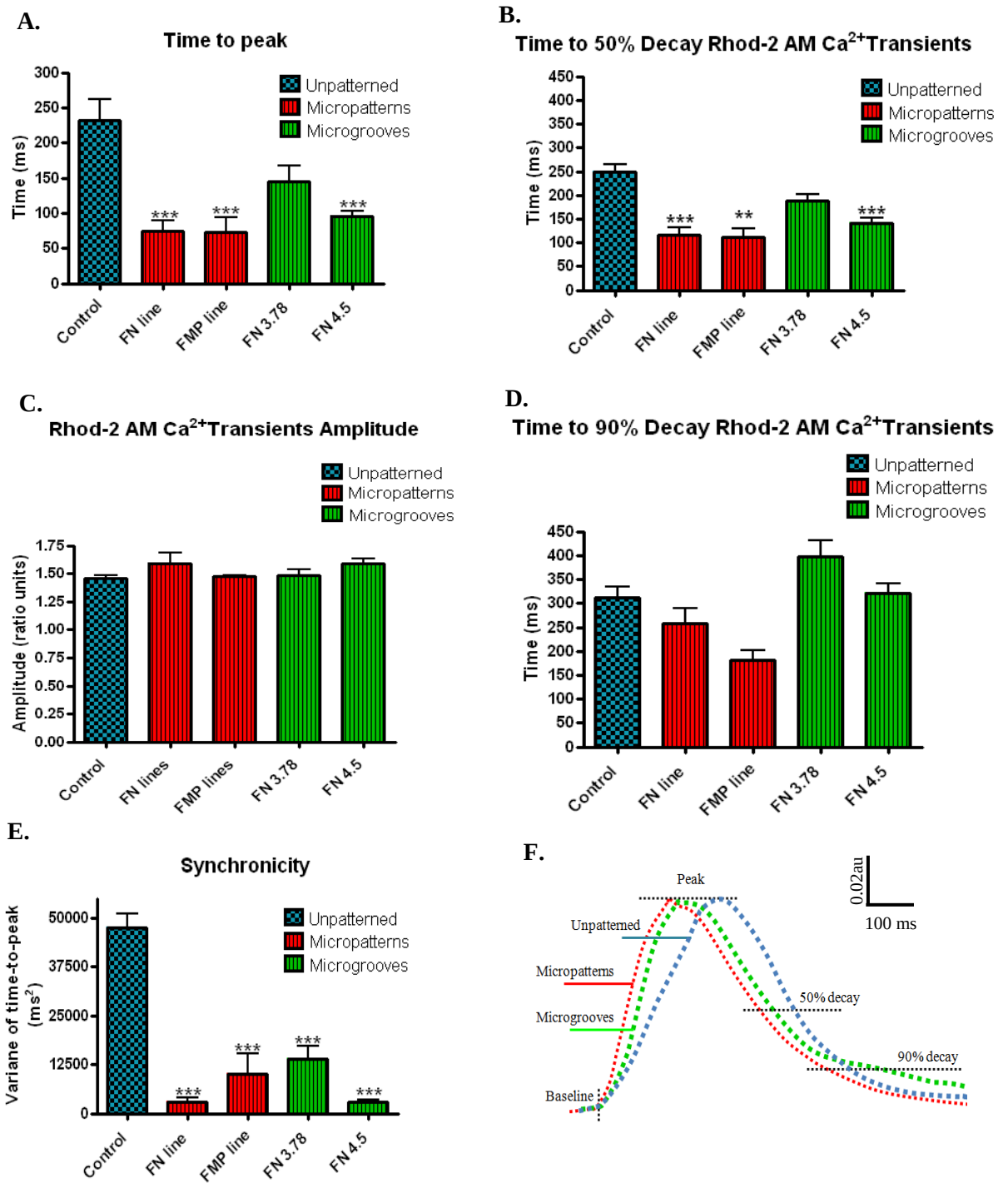

Figure 13. Rhod-2 AM fluorescence transient parameters.

A-E. Controlling cell structure by using PDMS scaffolds (FN coated microgrooves with 20-10µm W_1-W_2 and different depths 3.75 and 4.5µm, and FN and FMP micropatterns) affects Ca^{2+} handling vs control group, showing faster time-to-peak **(A)**, similar 50% decay **(B)**, no significant differences in amplitude **(C)**, niether 90% decay **(D)**, and smaller variance of time-to-peak **(E)**. **F.** Schematic records of Rhod-2 AM fluorescence transients showing variations in Ca^{2+} parameters. (All data were compared with control, ***P*<0.001, ****P*<0.0001)

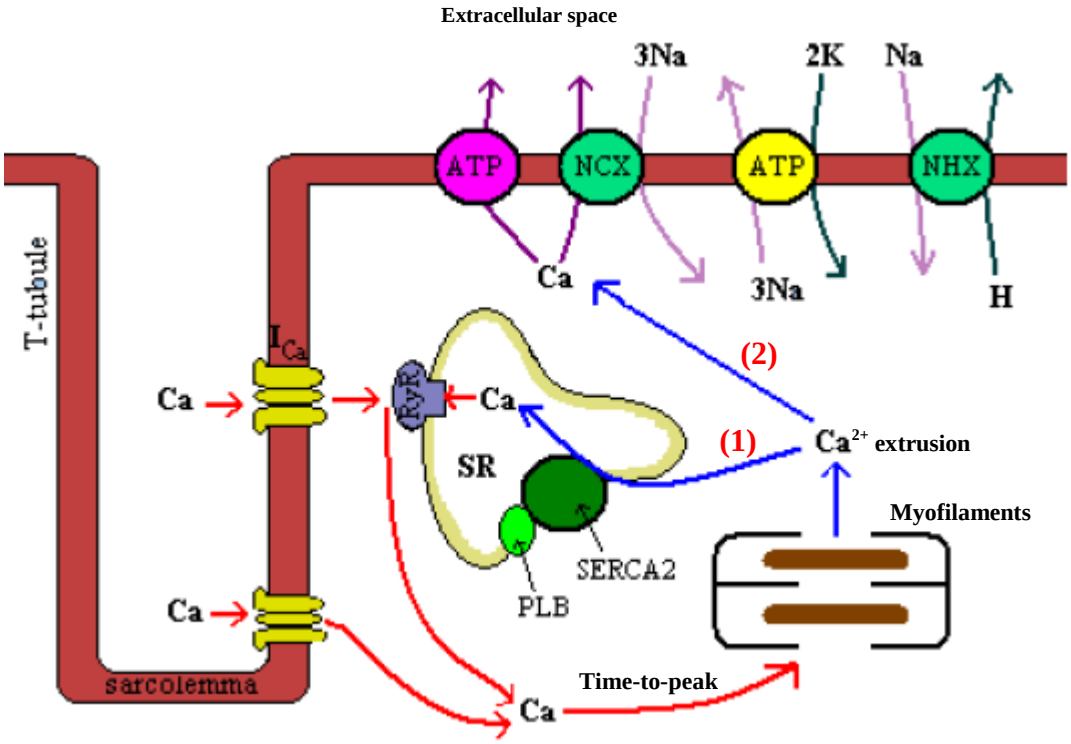

Figure 14. Simplified schematic illustration of Ca^{2+} handling mechanism.

The action potential arrives as a wave of depolarisation down the t-tubules to allow release of Ca^{2+} from the SR into the cystol. Ca^{2+} then binds to myofilaments and induces contraction. Following, cell repolarises and Ca^{2+} is extruded from the cystol into 1) SR via SERCA2 and 2) extracellular space via NCX.

	Seeded NRVMs		Ca^{2+} Transients Parameters					
			Time-to-peak (ms)	Synchronicity (ms^2)	Amplitude (F/F_0)	50% decay (ms)	90% decay (ms)	Heart beats (beat/minute)
Unaligned cells	Unpatterned	Control (n=12)	232.3±29.5	47.61±3.33	1.46±0.03	250±15.56	312.6±21.6	26
Aligned cells	Micropatterned PDMS	FN (n=9)	73.9±15.6	30.50±1.10	1.59±0.09	116.2±14.9	258.6±30.3	68
		FMP (n=4)	73.22±20.51	10.18±5.06	1.47±0.01	110.8±19.04	182.2±20.45	88
	Microgrooved PDMS	3.78µm (n=4)	144.7±22.5	14.07±3.17	1.48±0.05	188.3±12.8	398±34.16	65
		4.5µm (n=12)	96.08±6.31	29.91±4.74	1.59±0.03	141.8±11.27	321.9±18.57	70

Table 1. Ca^{2+} transient measurements during confocal experiments.